Reprinted from JOURNAL OF APPLIED PHYSICS, Vol. 36, No. 9, 2915–2924, September 1965

Slip-Induced Directional Order in Fe–Ni Alloys. I. Extension of the Chikazumi–Suzuki–Iwata Theory

G. Y. CHIN
Bell Telephone Laboratories, Incorporated, Murray Hill, New Jersey
(Received 4 February 1965)

In the present paper, calculations have been made for the magnetic anisotropy developed in cold-worked iron–nickel alloys near the 75% Ni composition. The treatment is based on the slip-induced directional order theory of Chikazumi *et al.* [J. Phys. Soc. Japan **12**, 1259 (1957)]. The theory states that in an ordered ferromagnetic solid solution (long- or short-range order, or clustering), slip results in the creation and preferential alignment of distinct type(s) of atom pairs (e.g., Fe–Fe) which lead to an induced magnetic anisotropy. The important conclusion from this theory is that the direction of the induced easy axis of magnetization depends sensitively on the orientation of the deforming crystal and the geometry of the deformation process, as well as the type and degree of ordering in the alloy. The present treatment extends the original analysis for the case of rolling to single crystals of several new orientations: (110)[$\bar{1}$12], (110)[$\bar{1}$10], (111)[$\bar{1}\bar{1}$2], (112)[$\bar{1}$10], and (112)[$\bar{1}\bar{1}$1]. These orientations, plus those studied by Chikazumi *et al.* ((100)[001], (100)[011], and (110)[001]), contain the most likely operating slip systems whose slip directions are symmetrically disposed about the rolling direction and are hence more stable than others during rolling. Some of these orientations are important components of texture in recrystallized or cold-rolled polycrystalline face-centered cubic materials. In addition to the rolling analysis, calculations have been made for the anisotropy resulting from drawing of wires with ⟨111⟩ and ⟨001⟩ axial orientations. These two orientations are likewise prominent components of polycrystalline wire textures.

The present work shows that drawing of a ⟨001⟩ wire induces a hard magnetic direction along the wire axis, while this axis becomes an easy direction if the orientation is ⟨111⟩. For rolling, except for the cases of (001)[100] and (110)[001] studied by Chikazumi *et al.*, where the induced easy axis lies along the transverse direction, most other orientations generally place the easy axis along the rolling direction. This suggests a plausible explanation for the observation that the rolling direction becomes an easy axis of magnetization when a randomly oriented polycrystalline aggregate is rolled. This work also predicts that rolling of {112}⟨111⟩ and {110}⟨112⟩ textures (symmetrical variants included), which are prominent texture components in rolled Permalloy, results in an easy axis along the rolling direction. Suggestions for experimental testing of the theory are discussed.

INTRODUCTION

THE phenomenon of cold-work induced magnetic anisotropy in iron–nickel alloys has been studied in detail in connection with the early development of Isoperm, a 50% Fe–50% Ni alloy.[1–3] It was found that rolling of a cube-textured alloy induces an "easy" axis of magnetization along the transverse direction. The induced easy axis lies along the rolling direction, however, if the initial grain orientation were random. This phenomenon was found to exist throughout the face-centered cubic range (at room temperature) of the Fe–Ni system and was unrelated to magnetostriction or crystalline anisotropy. Bunge and Mueller[4] and Chikazumi, Suzuki, and Iwata[5] (hereafter called CSI) proposed a slip-induced directional order theory to account for this peculiar anisotropy. Briefly, the theory states that in a ferromagnetic alloy containing some degree of chemical order (long or short range), there are more unlike nearest-neighbor atom pairs than in a random solid solution. During plastic deformation, like-atom pairs are created at the expense of unlike pairs.[6] Due to the crystallographic nature of slip, these induced like-atom pairs are distributed asymmetrically. Such asymmetrical distribution results in a magnetic anisotropy since it is expected from the theory of magnetic annealing[7,8] that the pseudodipolar magnetic coupling energy of an atom pair in a solid solution of A and B atoms depends on the identity of the pair; that is AA, BB, or AB. In this manner, Bunge and Mueller accounted qualitatively for the directional dependence of slip-induced anisotropy in rolling both randomly oriented and cube-textured materials. The treatment of CSI was more complete. They considered the difference in slip behavior between long- and short-range-ordered structures and analyzed the slip systems operating to accommodate the rolling deformation. The calculations based on rolling single crystals of Permalloy (76% Ni–24%Fe) of several orientations were found in satisfactory agreement with observed magnetic data. Later work on Fe_3Al[9] and Ni–Co alloys[10] again produced satisfactory results.

[1] W. H. Six, J. L. Snoek, and W. G. Burgers, De Ingenier **49**, E 195 (1934).
[2] H. W. Conradt, O. Dahl, and K. Sixtus, Z. Metallk. **32**, 231 (1940).
[3] G. W. Rathenau and J. L. Snoek, Physica **8**, 555 (1941).
[4] H. J. Bunge and H. G. Mueller, Z. Metallk. **48**, 26 (1957).
[5] S. Chikazumi, K. Suzuki, and H. Iwata, J. Phys. Soc. Japan **12**, 1259 (1957).
[6] The theory is equally applicable to the case of clustering in which atoms prefer like neighbors. Plastic deformation would then result in unlike atom pairs at the expense of like ones.
[7] L. Neel, J. Phys. Radium **15**, 225 (1954).
[8] S. Taniguchi and M. Yamamoto, Sci. Rept. Res. Inst. Tohoku Univ. **A6**, 330 (1954).
[9] S. Chikazumi, K. Suzuki, and H. Iwata, J. Phys. Soc. Japan **15**, 250 (1960).
[10] N. Tamagawa, Y. Nakagawa, and S. Chikazumi, J. Phys. Soc. Japan **17**, 1256 (1962).

It should be pointed out that Neel[7] has also interpreted the cold-work induced anisotropy on the basis of directional order theory. He suggested, however, that the ordering is a result of the large applied stresses coupled with diffusion enhanced by plastic deformation. This theory was criticized by Bunge and Mueller on grounds that the Bauschinger effect had to be invoked to explain the difference in the directional dependence of the induced easy axis between randomly oriented and cube-textured polycrystalline materials.

This paper extends the CSI analysis to rolling crystals of several new orientations of $FeNi_3$ composition, with particular emphasis on those orientations encountered in textured polycrystalline materials. In addition, since slip-induced directional order need not be restricted to rolling deformation, analyses were made for the case of wire-drawing. The present aim is twofold. First, since the CSI analysis predicts different directions for the induced easy axis depending on the crystal orientation and the type of deformation processing, study of a wide range of orientations and different types of deformation processing will further test the theory. Secondly, commercial fabrication of magnetic alloy components often entails a series of complicated thermal and mechanical treatments. As different textures may be developed by these treatments, their effects on the magnetic anisotropy of the finished product can be overriding and must not be ignored.

CHIKAZUMI–SUZUKI–IWATA ANALYSIS

The magnetic energy density of an alloy crystal of A and B atoms, due to creation of BB atom pairs induced by slip, can be written as

$$E=l\sum_i N_{BBi}\cos^2\varphi_i, \tag{1}$$

where $l=l_{AA}+l_{BB}-2l_{AB}$, with l_{AA}, l_{BB}, and l_{AB} as the coefficients of pseudodipolar coupling of AA, BB, and AB atom pairs. N_{BBi} is the number of BB pairs per unit volume created by the slip on slip system i, and φ_i is the angle between the local magnetization vector and the induced BB pair direction due to the ith slip system.

In calculating the distribution of induced BB pairs, CSI distinguished two types of deformation: (1) deformation of a long-range-ordered lattice with slip confined within the ordered domains and (2) deformation of a short-range-ordered lattice, or of a long-range-ordered lattice with slip extending beyond the domain boundaries. In the following these will be denoted as L.F. and S.C. types, respectively, in accordance with the original notation. The essential difference between the two types is that, for alloys of face-centered cubic structure which usually slip on {111} planes and along ⟨110⟩ directions, the induced BB pair direction (for a given slip system) in L.F. deformation is that ⟨110⟩ direction perpendicular to the slip direction. In the S.C. deformation, the slip plane normal becomes the effective induced BB pair direction. The expressions for the induced magnetic energy density according to these two types of deformation have been derived in the original paper and will not be repeated here. The results for a Ni–25%Fe alloy are

$$E_{\mathrm{LF}}=\tfrac{1}{8}K_{\mathrm{LF}}\sum_i |S_i|\,(\alpha_1\beta_{1i}+\alpha_2\beta_{2i}+\alpha_3\beta_{3i})^2, \tag{2}$$

$$E_{\mathrm{SC}}=\tfrac{1}{16}K_{\mathrm{SC}} \times\sum_i |S_i|\,(n_{2i}n_{3i}\alpha_2\alpha_3+n_{3i}n_{1i}\alpha_3\alpha_1+n_{1i}n_{2i}\alpha_1\alpha_2), \tag{3}$$

where

$K_{\mathrm{LF}}=Nlp_0p's^2$

$K_{\mathrm{SC}}=Nlp'\sigma$

N = number of atoms per unit volume.

$Nl\sim 3.1\times 10^8$ erg/cc for Fe–Ni alloys.[5]

p_0 = probability that a dislocation will not be paired with another to form a superdislocation.

p' = probability of one dislocation passed per atomic (slip) plane.

s = Bragg and Williams long-range-order parameter.

σ = Bethe short-range-order parameter.

$\alpha_{1,2,3}$ = direction cosines of the local magnetization vector with respect to the cubic axes of the crystal.

$\beta_{1i,2i,3i}$ = direction cosines of the induced BB pair direction for slip system i.

$n_{1i,2i,3i}$ = direction cosines of the slip plane normal for slip system i.

S_i = "slip density," or effective number of dislocations passed per atomic (slip) plane; proportional to the macroscopic glide-shear produced by system i. See Appendix.

The terms inside the parentheses are merely the expanded expressions for the $\cos^2\varphi_i$ term in Eq. (1). As to the summation, it is carried over all operating slip systems i. For face-centered cubic alloys, there are a maximum of twelve {111} ⟨110⟩ slip systems. Which of these systems will operate depend on the crystal orientation and on the geometry of the deformation. Generally these are the systems which have the largest value of the factor for resolving the applied stresses on the slip plane and in the slip direction (Schmid factor), and which act in such a way so as to accommodate the imposed external shape change of the material. This shape change is expressed as six components of the macroscopic strain tensor ϵ_{ij}. Each of these components in turn can be expressed as a linear combination of glide-shears γ_i in the active slip systems. The values γ_i are then solved in terms of ϵ_{ij}. This practice follows the procedures of Taylor[11] and Bishop and Hill,[12,13] who made calculations on a polycrystalline material by assuming that the shape change of an individual grain is the same as that of the aggregate.

It may be noted that for an arbitrary macroscopic shape change, five of the six strain components are

[11] G. I. Taylor, J. Inst. Met. **62**, 307 (1938).
[12] J. F. W. Bishop and R. Hill, Phil. Mag. **42**, 1298 (1951).
[13] J. F. W. Bishop, Phil. Mag. **44**, 51 (1953).

TABLE I. Values of ϵ, β, and n (referred to the cubic axes) for the twelve {111} ⟨110⟩ slip systems.

No. of slip system	Slip plane	Slip direction	$2\epsilon_{xx}$	$2\epsilon_{yy}$	$2\epsilon_{zz}$	$4\epsilon_{yz}$	$4\epsilon_{zx}$	$4\epsilon_{xy}$	$\sqrt{2}\beta_1$	$\sqrt{2}\beta_2$	$\sqrt{2}\beta_3$	$\sqrt{3}n_1$	$\sqrt{3}n_2$	$\sqrt{3}n_3$
1	(111)	$[0\bar{1}1]$	0	$-S_1$	S_1	0	S_1	$-S_1$	0	1	1	1	1	1
2	(111)	$[\bar{1}01]$	$-S_2$	0	S_2	S_2	0	$-S_2$	1	0	1	1	1	1
3	(111)	$[1\bar{1}0]$	S_3	$-S_3$	0	$-S_3$	S_3	0	1	1	0	1	1	1
4	$(11\bar{1})$	[101]	S_4	0	$-S_4$	S_4	0	S_4	1	0	−1	1	1	−1
5	$(11\bar{1})$	[011]	0	S_5	$-S_5$	0	S_5	S_5	0	1	−1	1	1	−1
6	$(11\bar{1})$	$[1\bar{1}0]$	S_6	$-S_6$	0	S_6	$-S_6$	0	1	1	0	1	1	−1
7	$(1\bar{1}1)$	[110]	S_7	$-S_7$	0	S_7	S_7	0	1	−1	0	1	−1	1
8	$(1\bar{1}1)$	$[\bar{1}01]$	$-S_8$	0	S_8	$-S_8$	0	S_8	1	0	1	1	−1	1
9	$(1\bar{1}1)$	[011]	0	$-S_9$	S_9	0	S_9	S_9	0	1	−1	1	−1	1
10	$(\bar{1}11)$	$[0\bar{1}1]$	0	$-S_{10}$	S_{10}	0	$-S_{10}$	S_{10}	0	1	1	−1	1	1
11	$(\bar{1}11)$	[101]	$-S_{11}$	0	S_{11}	S_{11}	0	S_{11}	1	0	−1	−1	1	1
12	$(\bar{1}11)$	[110]	$-S_{12}$	S_{12}	0	S_{12}	S_{12}	0	1	−1	0	−1	1	1

independent (the hydrostatic part being zero) and hence, at least five independent slip systems are required.[11–13] Under highly symmetrical conditions such as exist in the present analysis, however, this requirement can be relaxed.[14]

Values of ϵ_{ij}, together with those of β and n, for the twelve slip systems are given in Table I; cubic axes have been used as reference axes. Values of γ_i have been converted to S_i, the slip density expression in Eqs. (2) and (3). See Appendix for details. Table I essentially follows CSI's notation, with the sense of some slip directions changed so as to conform with the positive direction of the shears as written. Two sign errors in Table III of CSI's paper have also been corrected.

DETAILED CALCULATIONS

1. Wire Drawing

Wire textures of fcc metals and alloys are often a combination of ⟨001⟩ and ⟨111⟩ components; i.e., the grains have their ⟨001⟩ and ⟨111⟩ directions along the wire axis. Hence the effect of wire-drawing of crystals of these two orientations on the slip-induced anisotropy is of interest.

(a) *Drawing of a ⟨001⟩ crystal*

Let z be the [001] wire axis, and x and y be the [100] and [010] directions, respectively. The macroscopic strain components are:

$$\epsilon_{xx}=-r/2, \quad \epsilon_{yy}=-r/2, \quad \epsilon_{zz}=r,$$
$$\epsilon_{yz}=\epsilon_{zx}=\epsilon_{xy}=0, \tag{4}$$

where r is the reduction of area. Since wire drawing can be considered as tension along the wire axis,[15] Fig. 1 shows that four of the twelve slip systems, 3, 6, 7, and 12 (see Table I), do not operate because the slip directions are perpendicular to the [001] tensile axis. From Table I, the strain components in terms of the slip densities of the eight active slip systems are:

$$\begin{aligned}
2\epsilon_{xx}&=-S_2+S_4-S_8-S_{11},\\
2\epsilon_{yy}&=-S_1+S_5-S_9-S_{10},\\
2\epsilon_{zz}&=S_1+S_2-S_4-S_5+S_8+S_9+S_{10}+S_{11},\\
4\epsilon_{yz}&=S_2+S_4-S_8+S_{11},\\
4\epsilon_{zx}&=S_1+S_5+S_9-S_{10},\\
4\epsilon_{xy}&=-S_1-S_2+S_4+S_5+S_8+S_9+S_{10}+S_{11}.
\end{aligned} \tag{5}$$

From the symmetry of the slip systems, the $|S_i|$'s must be equal. Then solutions of Eqs. (4) and (5) give

$$S_1=S_2=S_8=S_9=S_{10}=S_{11}=r/4,$$
$$S_4=S_5=-(r/4).^{16} \tag{6}$$

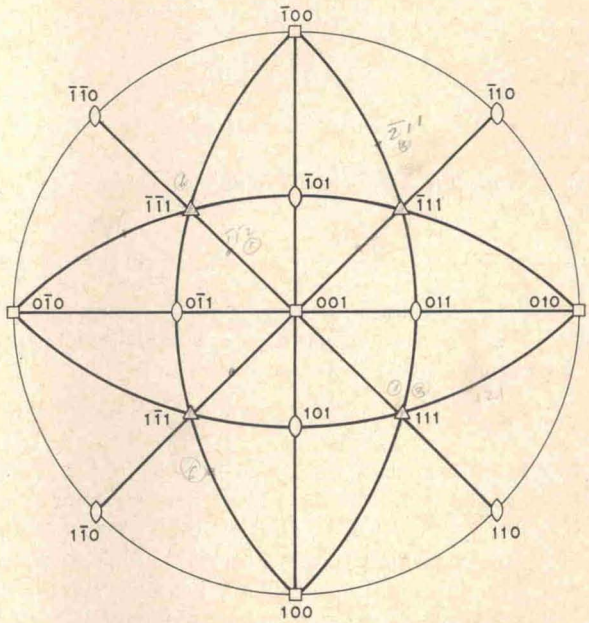

FIG. 1. Standard (001) stereographic projection of cubic crystal.

[14] M. R. Pickus and C. H. Mathewson, J. Inst. Metals **64**, 237 (1939).

[15] Although the stress system in wire-drawing probably consists of a tensile stress σ along the wire axis and a compressive stress $-n\sigma$ along two orthogonal axes in the radial direction, addition of a hydrostatic tension $n\sigma$ (which does not affect slip) will result in the equivalent system of a single tensile stress $(1+n)\sigma$ along the wire axis.

[16] For slip systems (4) and (5), the Miller indices for the slip plane in Table I are the negative of those of Fig. 1, resulting in the sign change of the shears. For simplicity, we shall consistently use the slip density values in Table I for slip systems whose Miller indices for plane or direction are the negative of those listed.

By putting Eq. (6) into (2) and using the pertinent values of β from Table I, one obtains for L.F. deformation

$$E_{LF}=(1/16)K_{LF}r(\alpha_1^2+\alpha_2^2+2\alpha_3^2)$$
$$=(1/16)K_{LF}r\alpha_3^2+\text{const.} \quad (7)$$

Since all values are positive, Eq. (7) means that the induced magnetic energy is a minimum on the x–y plane ($\alpha_3=0$). Hence the wire axis [001] becomes a hard axis of magnetization.

Substitution of Eq. (6) and the n values of Table I into Eq. (3) gives

$$E_{SC}=(1/16)K_{SC}[(r/4)\times 0]=0. \quad (8)$$

Hence there is no magnetic anisotropy produced by the S.C. type deformation.

(b) *Drawing of a ⟨111⟩ crystal*

Let x'–[$\bar{1}$10], y'–[$\bar{1}\bar{1}$2], and z'–[111] be a set of coordinate axes for the macroscopic strain tensor in this system; this retains the z' direction as the wire axis and the other two directions along the radial direction, Fig. 2. The matrix for the transformation of the specimen axes to the cubic axes referred to in Table I is[17]

	x'	y'	z'
X	$-\frac{1}{\sqrt{2}}$	$-\frac{1}{\sqrt{6}}$	$\frac{1}{\sqrt{3}}$
Y	$\frac{1}{\sqrt{2}}$	$-\frac{1}{\sqrt{6}}$	$\frac{1}{\sqrt{3}}$
Z	0	$\frac{2}{\sqrt{6}}$	$\frac{1}{\sqrt{3}}$.

Hence from the strain components for wire-drawing [Eq. (4)],

$$\epsilon_{x'x'}=\epsilon_{y'y'}=-r/2, \quad \epsilon_{z'z'}=r, \quad \epsilon_{y'z'}=\epsilon_{z'x'}=\epsilon_{x'y'}=0, \quad (9)$$

and the tensor relation $\epsilon_{ij}=l_{i'i}l_{j'j}\epsilon_{i'j'}$ ($i,j=x, y, z$; $i',j'=x', y', z'$)[18] where the l's are the components of the transformation matrix, one obtains

$$\epsilon_{xx}=\epsilon_{yy}=\epsilon_{zz}=0, \quad \epsilon_{yz}=\epsilon_{zx}=\epsilon_{xy}=r/2. \quad (10)$$

From the stereographic projection of Fig. 2, the operating slip systems for [$\bar{1}$11] wire drawing are (11$\bar{1}$) [101], (11$\bar{1}$) [011], (1$\bar{1}$1) [110], (1$\bar{1}$1) [011], ($\bar{1}$11) [101], and ($\bar{1}$11) [110], corresponding to Nos. 4, 5, 9, 11, and 12 of Table I. The other six systems are inoperative because of zero values of Schmid factor. From Table I, the strain components in terms of slip densities are:

$$2\epsilon_{xx}=S_4+S_7-S_{11}-S_{12},$$
$$2\epsilon_{yy}=S_5-S_7-S_9+S_{12},$$
$$2\epsilon_{zz}=-S_4-S_5+S_9+S_{11}, \quad (11)$$
$$4\epsilon_{yx}=S_4+S_7+S_{11}+S_{12},$$
$$4\epsilon_{zx}=S_5+S_7+S_9+S_{12},$$
$$4\epsilon_{xy}=S_4+S_5+S_9+S_{11}.$$

Solution of Eqs. (10) and (11) gives

$$S_4=S_5=S_7=S_9=S_{11}=S_{12}=r/2. \quad (12)$$

Putting (12) into (2) and using the β values of Table I, one obtains for L.F. deformation

$$E_{LF}=-\tfrac{1}{8}K_{LF}r(\alpha_1\alpha_2+\alpha_2\alpha_3+\alpha_3\alpha_1)+\text{const.} \quad (13)$$

Equation (13) is a minimum along [111], or the wire axis. Hence this axis becomes the induced easy axis of magnetization.

Substitution of (12) into (3) and using the n values of Table I gives

$$E_{SC}=-(1/48)K_{SC}r(\alpha_1\alpha_2+\alpha_2\alpha_3+\alpha_3\alpha_1). \quad (14)$$

Again the wire axis becomes the induced easy axis.

2. Rolling

Rolling of the following orientations are of interest:

	Roll plane	Roll direction
1.	(001)	[$\bar{1}$00]
2.	(001)	[$\bar{1}$10]
3.	(110)	[001]
4.	(110)	[$\bar{1}$12]
5.	(110)	[$\bar{1}$10]
6.	(111)	[$\bar{1}\bar{1}$2]
7.	(112)	[$\bar{1}$10]
8.	(112)	[$\bar{1}\bar{1}$1]

In all the orientations above, slip directions of the operating slip systems (based on maximum resolved shear stress) are symmetrically disposed about the rolling axis and hence comply with the stability criterion of Pickus and Mathewson.[14] [Orientations (6) and (7), however, were not considered in their discussion of stability.] Tucker[19] has pointed out, however, that the real test of stability is to determine whether slight displacements from a given orientation will cause rotation into, or away from, this orientation. In any case, the following analyses should be valid for rolling reductions in which the orientation does not change significantly. Moreover, by following the orientation change such as with x-ray techniques, the magnetic anisotropy according to the new orientation(s) may still be obtained. Among the above list, (001) [$\bar{1}$00] is a prominent recrystallization texture in face-centered cubic alloys, while (110) [$\bar{1}$12] and (112) [$\bar{1}\bar{1}$1] are often found in the rolled state.[20]

[17] J. F. Nye, *Physical Properties of Crystals* (Oxford University Press, London, 1960), p. 9.
[18] Ref. 17, p. 11.
[19] G. E. G. Tucker, J. Inst. Metals 82, 655 (1954).
[20] C. S. Barrett, *Structure of Metals* (McGraw-Hill Book Company, Inc., New York, 1952), pp. 484, 509.

Since the first three cases have been treated by CSI, only their results will be summarized later. The other cases are analyzed below.

(a) (110) [$\bar{1}12$] *Rolling*

Rolling can be considered as plane strain deformation, the strain components given by

$$\epsilon_{x'x'}=-r, \quad \epsilon_{y'y'}=0, \quad \epsilon_{z'z'}=r,$$
$$\epsilon_{y'z'}=\epsilon_{z'x'}=\epsilon_{x'y'}=0, \tag{15}$$

where x' is normal to the rolling plane, y' transverse to the rolling direction, and z' the rolling direction.

For the case of rolling on (110) along [$\bar{1}12$], let $x'-[110]$, $y'-[\bar{1}1\bar{1}]$, and $z'-[\bar{1}12]$ be the coordinate axes, Fig. 3. The matrix for transformation to the cubic axes is

	x'	y'	z'
X	$\frac{1}{\sqrt{2}}$	$-\frac{1}{\sqrt{3}}$	$-\frac{1}{\sqrt{6}}$
Y	$\frac{1}{\sqrt{2}}$	$\frac{1}{\sqrt{3}}$	$\frac{1}{\sqrt{6}}$
Z	0	$-\frac{1}{\sqrt{3}}$	$\frac{2}{\sqrt{6}}$.

From Eq. 15 and the transformation matrix, the strain components referred to cubic axes become

$$\epsilon_{xx}=-r/3, \quad \epsilon_{yy}=-r/3, \quad \epsilon_{zz}=2r/3,$$
$$\epsilon_{yz}=r/3, \quad \epsilon_{zx}=-r/3, \quad \epsilon_{xy}=-2r/3. \tag{16}$$

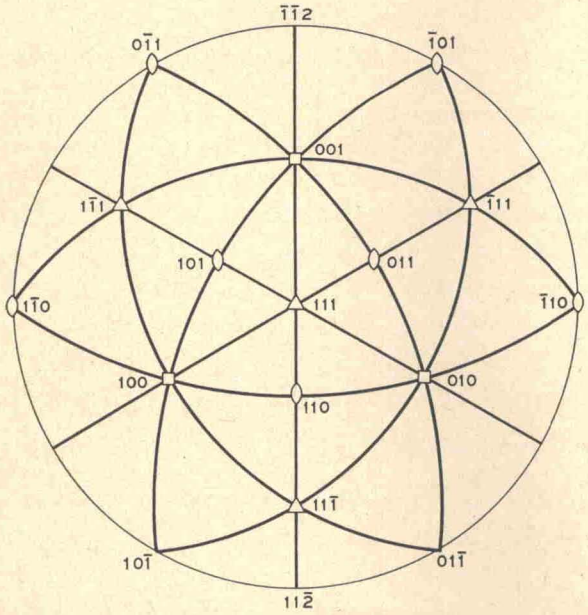

FIG. 2. Standard (111) stereographic projection of cubic crystal.

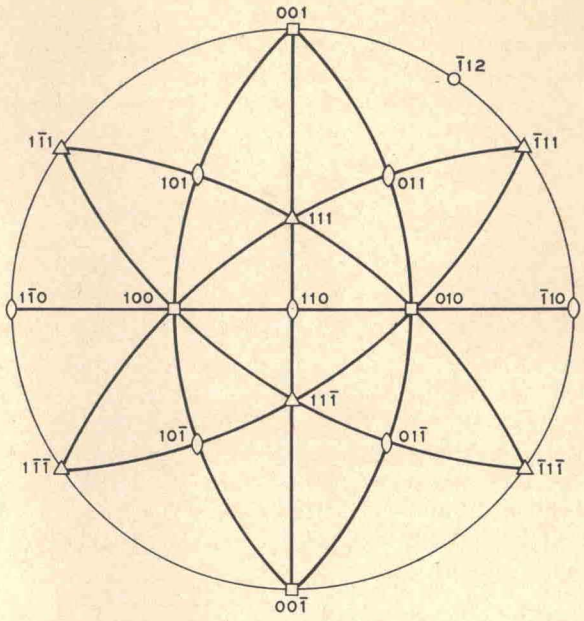

FIG. 3. Standard (110) stereographic projection of cubic crystal.

The choice of operating slip systems in rolling is complicated as the stress system is not simple. Pickus and Mathewson[14] chose those systems which have the largest value of $\cos\lambda\cos\theta\cos\varphi$, where λ and θ are the angles which the rolling plane normal makes with the slip plane normal and the slip direction, respectively; and φ is the angle between the slip direction and the rolling direction. Tucker[21] has proposed that the magnitudes of stress in rolling are σ along the rolling plane normal, $-n\sigma$ along the rolling direction, and $\frac{1}{2}(1-n)\sigma$ along the transverse direction, with $n<1$. The effective Schmid factor for a slip system is then proportional to $[(\cos\lambda\cos\theta)-(\cos\gamma\cos\varphi)]$, where γ is the angle between the slip plane normal and the rolling direction. The other symbols retain their previous meanings. Those slip systems with the largest effective Schmid factor will then operate. Although both criteria often lead to the choice of the same slip systems, it was felt that the Tucker approach is more appropriate and hence adopted here. In any event, the operating slip systems based on either stress criterion may be insufficient to accommodate the macroscopic strains. In such a case, additional slip on other systems may be required.[22]

From the stereographic projection of Fig. 3, the most likely slip systems that operate during (110) [$\bar{1}12$]

[21] G. E. G. Tucker, Acta Met. **12**, 1093 (1964).

[22] In the Bishop and Hill analysis,[12,13] one can obtain a sufficient number of slip systems to accommodate the imposed macroscopic strains while satisfying the yield criterion, i.e., the resolved shear stress for slip is reached equally in all the operating slip systems. With reference to the operating slip systems analyzed in the present paper using the Tucker approach, a recent calculation[23] based on the Bishop and Hill analysis yields the same results.

[23] G. Y. Chin, E. A. Nesbitt, and A. J. Williams, Acta Met. (to be published).

rolling are (111) [10$\bar{1}$] and (11$\bar{1}$) [011] which are in accord with both the criteria of Tucker and of Pickus and Mathewson. These are systems Nos. (2) and (5) according to Table I. The strain components in terms of slip density are:

$$2\epsilon_{xx}=-S_2, \quad 2\epsilon_{yy}=S_5, \quad 2\epsilon_{zz}=S_2-S_5,$$
$$4\epsilon_{yz}=S_2, \quad 4\epsilon_{zx}=S_5, \quad 4\epsilon_{xy}=-S_2+S_5. \quad (17)$$

Solution of Eqs. (16) and the normal strain equations of (17) gives

$$S_2=\tfrac{2}{3}r, \quad S_5=-\tfrac{2}{3}r, \quad (18)$$

which, however, do not satisfy the shear-strain equations of (17). In this case, other slip systems may be forced to act. Since [011] and [10$\bar{1}$] are the only pair of slip directions symmetrical to the specimen coordinate axes, the most likely slip systems to act are (1$\bar{1}$1) [10$\bar{1}$] and (1$\bar{1}$1) [011] [Nos. (8) and (9), respectively] in addition to Nos. (2) and (5). The strain components then become

$$\begin{aligned}
2\epsilon_{xx}&=-S_2-S_8,\\
2\epsilon_{yy}&=S_5-S_9,\\
2\epsilon_{zz}&=S_2-S_5+S_8+S_9,\\
4\epsilon_{yz}&=S_2-S_8,\\
4\epsilon_{zx}&=S_5+S_9,\\
4\epsilon_{xy}&=-S_2+S_5+S_8+S_9.
\end{aligned} \quad (19)$$

Solution of Eqs. (16) and (19) gives

$$S_2=r, \quad S_5=-r, \quad S_8=S_9=-(r/3) \quad (20)$$

with all the strain components satisfied. It may be noted that systems (8) and (9) are in cross-slip relationship (sharing the same slip direction) with systems (2) and (5), respectively, and that the amount of slip required of (8) and (9) is only one-third that of (2) and (5).

Although the Schmid factor is zero for systems (8) and (9), local stress variations may generate sufficient slip to satisfy the macrostrains. Alternatively, slip may still occur predominantly in systems (2) and (5) with resultant shape changes other than those prescribed by Eq. (15). Both modes of deformation are considered below.

On the assumption that only slip systems (2) and (5) operate, the induced anisotropy energy for L.F. deformation, according to Eqs. (2) and (18) and Table I, is

$$\begin{aligned}
E_{\mathrm{LF}}&=\tfrac{1}{8}K_{\mathrm{LF}}[\tfrac{2}{3}r(\tfrac{1}{2}\alpha_1^2+\tfrac{1}{2}\alpha_2^2+\alpha_3^2-\alpha_3\alpha_2+\alpha_3\alpha_1)]\\
&=(1/24)K_{\mathrm{LF}}r(\alpha_3^2-2\alpha_3\alpha_2+2\alpha_3\alpha_1)+\text{const.}
\end{aligned} \quad (21)$$

For magnetic torque and hysteresis loop measurements, it is more convenient to confine the anisotropy to the rolling plane. On the (110) rolling plane, Eq. (21) indicates that the easy direction is [$\bar{1}$11], which is 19.5° from the [$\bar{1}$12] rolling direction, Fig. 3.

For S.C. deformation, Eqs. (3) and (20) and Table I give

$$E_{\mathrm{SC}}=\tfrac{1}{16}K_{\mathrm{SC}}(\tfrac{2}{3}r)(\tfrac{2}{3}\alpha_1\alpha_2)=(1/36)K_{\mathrm{SC}}r\alpha_1\alpha_2. \quad (22)$$

E_{SC} is thus minimum along [$\bar{1}$10] which is 55° from the [$\bar{1}$12] rolling direction. If slip systems (2), (5), (8), and (9) all operate,

$$E_{\mathrm{LF}}=(5/48)K_{\mathrm{LF}}r(\alpha_3^2-2\alpha_3\alpha_2+2\alpha_3\alpha_1)+\text{const.}, \quad (23)$$

which again places the easy direction along [$\bar{1}$11]. For S.C. deformation,

$$\begin{aligned}
E_{\mathrm{SC}}&=(1/24)K_{\mathrm{SC}}r\alpha_1\alpha_2\\
&\quad+(1/72)K_{\mathrm{SC}}r(-\alpha_2\alpha_3+\alpha_3\alpha_1-\alpha_1\alpha_2)\\
&=(1/72)K_{\mathrm{SC}}r(2\alpha_1\alpha_2-\alpha_2\alpha_3+\alpha_3\alpha_1).
\end{aligned} \quad (24)$$

A calculation based on Eq. (24) shows that on the (110) plane, the easy direction is near [$\bar{1}$11] and about 25° from the [$\bar{1}$12] rolling direction.

(*b*) (*110*) [$\bar{1}$*10*] *Rolling*

Let x'−[110], y'−[00$\bar{1}$], and z'−[$\bar{1}$10] be the coordinate axes, Fig. 3. The matrix for the transformation to cubic axes is

	x'	y'	z'
x	$\frac{1}{\sqrt{2}}$	0	$-\frac{1}{\sqrt{2}}$
y	$\frac{1}{\sqrt{2}}$	0	$\frac{1}{\sqrt{2}}$
z	0	−1	0.

From Eq. (15) and the transformation matrix, the strain components referred to cubic axes become

$$\epsilon_{xx}=\epsilon_{yy}=\epsilon_{zz}=\epsilon_{yz}=\epsilon_{zx}=0, \quad \epsilon_{xy}=-r. \quad (25)$$

The most likely slip systems to operate are Nos. (1), (2), (4), (5), (8), (9), (10), and (11) according to the Tucker criterion. [Only (1), (2), (4), and (5) are chosen according to the criterion of Pickus and Mathewson.] In this case

$$\begin{aligned}
2\epsilon_{xx}&=-S_2+S_4-S_8-S_{11},\\
2\epsilon_{yy}&=-S_1+S_5-S_9-S_{10},\\
2\epsilon_{zz}&=S_1+S_2-S_4-S_5+S_8+S_9+S_{10}+S_{11},\\
4\epsilon_{yx}&=S_2+S_4-S_8+S_{11},\\
4\epsilon_{zx}&=S_1+S_5+S_9-S_{10},\\
4\epsilon_{xy}&=-S_1-S_2+S_4+S_5+S_8+S_9+S_{10}+S_{11}.
\end{aligned} \quad (26)$$

Solution of Eqs. (25) and (26) gives

$$S_1=S_2=r/2, \ S_4=S_5=S_8=S_9=S_{10}=S_{11}=-(r/2), \quad (27)$$

with the result that

$$E_{\mathrm{LF}}=\tfrac{1}{8}K_{\mathrm{LF}}r\alpha_3^2+\text{const.} \quad (28)$$

and

$$E_{\mathrm{SC}}=0. \quad (29)$$

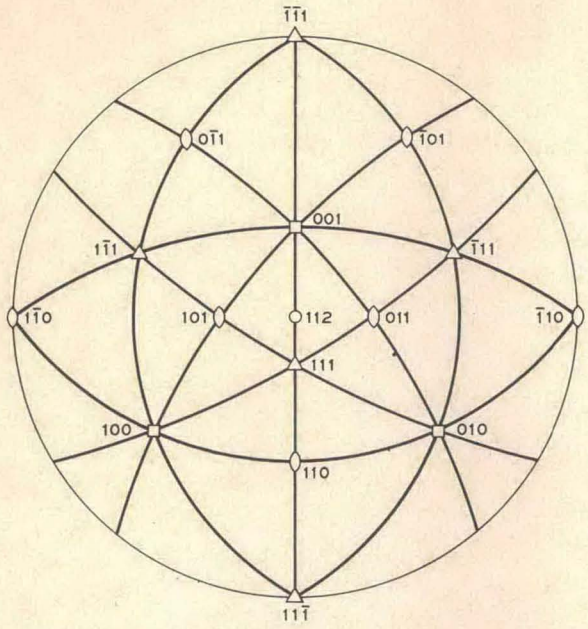

FIG. 4. Standard (112) stereographic projection of cubic crystal.

Eq. (28) means that the [001] is a hard direction for L.F. deformation, so that the easy direction on the (110) plane is along the $[\bar{1}10]$ rolling direction. There is no anisotropy from S.C. deformation, Eq. (29).

(c) (111) $[\bar{1}\bar{1}2]$ *Rolling*

The specimen coordinate system specifies $x'-[111]$, $y'-[\bar{1}10]$, and $z'-[\bar{1}\bar{1}2]$. The transformation matrix is

	x'	y'	z'
X	$\frac{1}{\sqrt{3}}$	$-\frac{1}{\sqrt{2}}$	$-\frac{1}{\sqrt{6}}$
Y	$\frac{1}{\sqrt{3}}$	$\frac{1}{\sqrt{2}}$	$-\frac{1}{\sqrt{6}}$
Z	$\frac{1}{\sqrt{3}}$	0	$\frac{2}{\sqrt{6}}$.

Hence

$$\epsilon_{xx}=-r/6, \quad \epsilon_{yy}=-r/6, \quad \epsilon_{zz}=r/3,$$
$$\epsilon_{yz}=\epsilon_{zx}=-2r/3, \quad \epsilon_{xy}=-r/6. \tag{30}$$

From Fig. 2, the active slip systems based on the Tucker criterion are (4), (5), (7), and (12). Then

$$\begin{aligned} 2\epsilon_{xx}&=S_4+S_7-S_{12},\\ 2\epsilon_{yy}&=S_5-S_7+S_{12},\\ 2\epsilon_{zz}&=-S_4-S_5,\\ 4\epsilon_{yz}&=S_4+S_7+S_{12},\\ 4\epsilon_{zx}&=S_5+S_7+S_{12},\\ 4\epsilon_{xy}&=S_4+S_5. \end{aligned} \tag{31}$$

Solution of (30) and (31) gives

$$S_4=S_5=-(r/3), \quad S_7=S_{12}=-(7/6)r. \tag{32}$$

Hence

$$E_{\mathrm{LF}}=(1/48)K_{\mathrm{LF}}r[(\alpha_3^2-\alpha_2\alpha_3-\alpha_3\alpha_1)+7(\alpha_1-\alpha_2)^2]. \tag{33}$$

The second term inside the brackets dominates and places the hard direction at $[\bar{1}10]$, which is transverse to the $[\bar{1}\bar{1}2]$ rolling direction. Similarly,

$$E_{\mathrm{SC}}=-(1/144)K_{\mathrm{SC}}r(2\alpha_2\alpha_3+2\alpha_3\alpha_1+5\alpha_1\alpha_2). \tag{34}$$

Calculation based on Eq. (34) shows that the hard direction on the rolling plane is again $[\bar{1}10]$.

(d) (112) $[\bar{1}10]$ *Rolling*

The specimen coordinate axes are: $x'-[112]$, $y'-[11\bar{1}]$, and $z'-[\bar{1}10]$, Fig. 4. The transformation matrix is

	x'	y'	z'
X	$\frac{1}{\sqrt{6}}$	$\frac{1}{\sqrt{3}}$	$-\frac{1}{\sqrt{2}}$
Y	$\frac{1}{\sqrt{6}}$	$\frac{1}{\sqrt{3}}$	$\frac{1}{\sqrt{2}}$
Z	$\frac{2}{\sqrt{6}}$	$-\frac{1}{\sqrt{3}}$	0 .

Hence

$$\epsilon_{xx}=r/3, \quad \epsilon_{yy}r/3, \quad \epsilon_{zz}=-2r/3,$$
$$\epsilon_{yz}=-r/3, \quad \epsilon_{zx}=-r/3, \quad \epsilon_{xy}=-2r/3. \tag{35}$$

Although Fig. 4 shows that $(1\bar{1}1)$ [011] and $(\bar{1}11)$ [101] [Nos. (9) and (11)] are the most likely systems to operate according to the Tucker criterion, they are not enough to satisfy the strain equations (35). Additional slip on the cross-slip systems $(11\bar{1})$ [101] and $(11\bar{1})$ [011] [Nos. (4) and (5)] may then be assumed. Thus

$$\begin{aligned} 2\epsilon_{xx}&=S_4-S_{11},\\ 2\epsilon_{yy}&=S_5-S_9,\\ 2\epsilon_{zz}&=-S_4-S_5+S_9+S_{11},\\ 4\epsilon_{yz}&=S_4+S_{11},\\ 4\epsilon_{zx}&=S_5+S_9,\\ 4\epsilon_{xy}&=S_4+S_5+S_9+S_{11}. \end{aligned} \tag{36}$$

Solution of Eqs. (35) and (36) gives

$$S_4=S_5=-(r/3), \quad S_9=S_{11}=r. \tag{37}$$

Hence

$$E_{\mathrm{LF}}=(1/48)K_{\mathrm{LF}}r(3\alpha_3^2-7\alpha_2\alpha_3-7\alpha_3\alpha_1). \tag{38}$$

On the rolling (112) plane, E_{LF} is minimum along the $[\bar{1}10]$ rolling direction. Likewise,

$$E_{\mathrm{SC}}=-(1/72)K_{\mathrm{SC}}r(\alpha_2\alpha_3+\alpha_3\alpha_1+2\alpha_1\alpha_2). \tag{39}$$

TABLE II. Summary of calculated anisotropy energies based on slip-induced directional order theory.

A. Wire drawing WA	E_{LF}	Easy axis	E_{SC}	Easy axis
1. ⟨001⟩	$(K_{LF}r/16)\alpha_3^2$	⊥WA	0	···
2. ⟨111⟩	$-(K_{LF}r/8)(\alpha_1\alpha_2+\alpha_2\alpha_3+\alpha_3\alpha_1)$	WA	$-(K_{SC}r/48)(\alpha_1\alpha_2+\alpha_2\alpha_3+\alpha_3\alpha_1)$	WA

B. Rolling RP RD		E_{LF}	Easy axis on RP		E_{SC}	Easy axis on RP
1. (001)[100][a]	a.	$-(K_{LF}r/8)\alpha_2^2$	TD	a.	0	···
	b.	$-(K_{LF}r/8)\alpha_2^2$	TD	b.	$(K_{SC}r/24)\alpha_2\alpha_3$	~TD
2. (001)[110][a]	a.	$(K_{LF}r/16)\alpha_3^2$	···	a.	$(K_{SC}r/24)\alpha_1\alpha_2$	TD
	b.	$-(K_{LF}r^2/4)\cos^2\theta$	RD	b.	$[K_{SC}r(1-2r)/24]\cos^2\theta$	TD
3. (110)[001][a]	a.	$(K_{LF}r/16)\alpha_3^2$	TD	a.	$(K_{SC}r/24)\alpha_1\alpha_2$	TD
	b.	$(K_{LF}r/16)\alpha_3^2$	TD	b.	$(K_{SC}r/24)\alpha_1\alpha_2$	TD
4. (110)[$\bar{1}$12][b]	a.	$(K_{LF}r/24)[(\alpha_1+\alpha_3)^2+(\alpha_2-\alpha_3)^2]$	[$\bar{1}$11], 20° from RD	a.	$(K_{SC}r/36)\alpha_1\alpha_2$	[$\bar{1}$10], 55° from RD
	b.	$(5K_{LF}r/48)[(\alpha_1+\alpha_3)^2+(\alpha_2-\alpha_3)^2]$	[$\bar{1}$11], 20° from RD	b.	$(K_{SC}r/72)(2\alpha_1\alpha_2-\alpha_2\alpha_3+\alpha_3\alpha_1)$	near [$\bar{1}$11], 25° from RD
5. (110)[$\bar{1}$10]		$(K_{LF}r/8)\alpha_3^2$	RD		0	···
6. (111)[$\bar{1}\bar{1}$2]		$\sim(7K_{LF}r/48)(\alpha_1-\alpha_2)^2$	RD		$-(K_{SC}r/144)(2\alpha_2\alpha_3+2\alpha_3\alpha_1+5\alpha_1\alpha_2)$	RD
7. (112)[$\bar{1}$10][b]	a.	$(K_{LF}r/24)(\alpha_3^2-2\alpha_2\alpha_3-2\alpha_3\alpha_1)$	RD	a.	$-(K_{SC}r/36)\alpha_1\alpha_2$	TD
	b.	$(K_{LF}r/48)(3\alpha_3^2-7\alpha_2\alpha_3-7\alpha_3\alpha_1)$	RD	b.	$-(K_{SC}r/72)(\alpha_2\alpha_3+\alpha_3\alpha_1+2\alpha_1\alpha_2)$	TD
8. (112)[$\bar{1}\bar{1}$1]		$(K_{LF}r/48)[(\alpha_1+\alpha_3)^2+(\alpha_2+\alpha_3)^2+7(\alpha_1-\alpha_2)^2]$	RD		$(K_{SC}r/144)(2\alpha_2\alpha_3+2\alpha_3\alpha_1-5\alpha_1\alpha_2)$	RD

[a] These three cases have been analyzed and studied by CSI.[5] a, calculation based on homogeneous slip; b, based on observed slip.
[b] a, calculation based on slip on systems of maximum effective Schmid factor; b, based on additional slip systems to achieve strain compatibility. WA wire axis; RP, rolling plane; RD, rolling direction; TD, transverse direction.

On the (112) plane, E_{SC} is maximum along [$\bar{1}$10]. Hence this anisotropy opposes that obtained from L.F. deformation. If only systems (9) and (11) operate, despite strain incompatibility,

$$E_{LF}=(1/24)K_{LF}r(\alpha_3^2-2\alpha_2\alpha_3-2\alpha_3\alpha_1) \quad (40)$$

and

$$E_{SC}=-(1/36)K_{SC}r\alpha_1\alpha_2. \quad (41)$$

The predicted easy directions on (112) are thus the same as the four slip system case.

(e) (112) [$\bar{1}\bar{1}$1] Rolling

The specimen coordinate axes are now x'−[112], y'−[$\bar{1}$10], and z'−[$\bar{1}\bar{1}$1], Fig. 4. The transformation matrix is

	x'	y'	z'
x	$\frac{1}{\sqrt{6}}$	$-\frac{1}{\sqrt{2}}$	$-\frac{1}{\sqrt{3}}$
y	$\frac{1}{\sqrt{6}}$	$\frac{1}{\sqrt{2}}$	$-\frac{1}{\sqrt{3}}$
z	$\frac{2}{\sqrt{6}}$	0	$\frac{1}{\sqrt{3}}$

and

$$\epsilon_{xx}=r/6,\quad \epsilon_{yy}=r/6,\quad \epsilon_{zz}=-r/3,$$
$$\epsilon_{yx}=-2r/3,\quad \epsilon_{zx}=-2r/3,\quad \epsilon_{xy}=r/6. \quad (42)$$

The operating slip systems are most likely (111) [0$\bar{1}$1], (111) [$\bar{1}$01], (1$\bar{1}$1) [110], and ($\bar{1}$11) [110], or Nos. (1), (2), (7), and (12). Then

$$\begin{aligned}
2\epsilon_{xx}&=-S_2+S_7-S_{12},\\
2\epsilon_{yy}&=-S_1-S_7+S_{12},\\
2\epsilon_{zz}&=S_1+S_2,\\
4\epsilon_{yz}&=S_2+S_7+S_{12},\\
4\epsilon_{zx}&=S_1+S_7+S_{12},\\
4\epsilon_{xy}&=-S_1-S_2.
\end{aligned} \quad (43)$$

Solution of Eqs. (42) and (43) gives

$$S_1=S_2=-(r/3),\quad S_7=S_{12}=-(7/6)r. \quad (44)$$

Hence

$$E_{LF}=(1/48)K_{LF}r[(\alpha_1+\alpha_3)^2+(\alpha_2+\alpha_3)^2+7(\alpha_1-\alpha_2)^2]. \quad (45)$$

Equation (45) tells us that on the (112) rolling plane the [$\bar{1}\bar{1}$1] direction (rolling direction) is the easy axis. Similarly,

$$E_{SC}=(1/144)K_{SC}r(2\alpha_2\alpha_3+2\alpha_3\alpha_1-5\alpha_1\alpha_2), \quad (46)$$

which again places the easy direction at [$\bar{1}\bar{1}$1] as far as the (112) rolling plane is concerned.

DISCUSSION

The results of the preceding calculations are summarized in Table II, together with the three cases studied by Chikazumi *et al.*[5] The positions of the induced easy axis on the rolling plane are indicated. These positions are perhaps the most significant predictions of the theory, for they can be checked conveniently by magnetic torque measurements on a disk

cut out of the rolling plane. A more quantitative check on the theory is difficult because not enough is known about the coefficients K_{LF} and K_{SC}. As discussed by Chikazumi *et al.*, parameters such as p_0 and p' are not very accessible to experimentation as they depend sensitively on the details of dislocation motion. In addition, the order parameters s and σ are expected to decrease with increasing deformation,[24,25] so that the integrated forms of Eqs. (2) and (3) may be required. Attempt at a quantitative study was made by CSI, but the results were inconclusive for the above reasons.

Regarding the effect of long- and short-range-order on the slip-induced anisotropy, cases (1), (4), (5), and (7) for rolling in Table II are of interest, since different directions of the easy axis are predicted depending on the type of order. At compositions close to 75% Ni, appropriate heat treatments may be used to bring about mainly one type of ordering. Or, short-range order may be achieved at the expense of long range by choosing the composition well away from the 75% Ni region. While the kinetics of long-range ordering is sluggish, short-range order appears unavoidable over a range of the Fe–Ni composition.[26] Although the above analyses were made for 75% Ni–25% Fe only, a change in composition would affect the number of induced atom pairs (hence K_{LF} and K_{SC}) but not their directions. Consequently the predicted positions of the easy directions outlined in Table II would still be applicable.

It is assumed in the present analysis that the choice of the operating slip systems is made on the basis of satisfying the macroscopic stress and strain conditions. Wire drawing has been considered as tension along the wire axis and rolling as a triaxial stress system with the symmetry directions as principal stress axes. In the two cases ((110) $[1\bar{1}2]$ and (112) $[1\bar{1}0]$) where the operating slip systems based on stress consideration do not satisfy strain compatibility, alternative analyses were made to provide for additional slip systems.

It is further assumed in the present analysis that all operating slip systems operate homogeneously throughout the sample. If certain systems exclude one another, for reasons such as unequal hardening and change in stress due to lattice reorientation during deformation, the resulting anisotropies may be different from those of Table II. In the CSI study, for example, systems (1), (2), (4), and (5) are predicted in (001) [110] rolling. Slip-line observations, however, show that systems (1) and (2) operate on the top side of the crystal and (4) and (5) on the bottom. Hence inhomogeneity of deformation may have to be considered in individual cases.

Aside from the above considerations, Table II presents several interesting conclusions. During wire drawing, for example, the wire axis becomes magnetically hard or easy depending on whether the orientation is ⟨001⟩ or ⟨111⟩. As for plane strain deformation, usually realized in rolling, most of the orientations predict the rolling direction as the induced easy axis, notable exceptions being (001) [100] and (110) [001]. The case of (110) $[\bar{1}12]$ rolling is also interesting since it predicts an easy axis other than the rolling or transverse direction, hence the theory can be put to a severe test here.

Table II also has implications for rolling polycrystalline materials. Since all the orientations described are symmetrical orientations (with respect to rolling), an initially randomly oriented grain probably rotates to one of these orientations after a small deformation. A majority of these orientations place the easy axis along the rolling direction; which may explain the observation that the rolling direction is the easy axis for an initially random polycrystalline aggregate of Permalloy.[2] In this connection, it is interesting to note that the rolling direction continues to be the easy axis at 90% thickness reduction or more where the texture is no longer random. The rolled texture in face-centered cubic Fe–Ni alloys can be described as (112) $[11\bar{1}]$ plus (110) $[\bar{1}12]$, the former component being the larger.[2] Table II reveals that rolling of a (112) $[11\bar{1}]$ crystal results in an easy axis along the rolling direction. As for the (110) $[\bar{1}12]$ texture, it actually consists of two symmetrical components, which may be written as (110) $[\bar{1}12]+(110)$ $[1\bar{1}2]$. Hence the anisotropy listed in Table II for (110) $[\bar{1}12]$ should be superposed onto that for (110) $[1\bar{1}2]$. When this is done, the effective easy axis is again most likely along the rolling direction.

Finally it should be noted that plane strain conditions can be approximated by processes other than rolling. Two cases of technological importance are wire flattening by rolling and flat-drawing. These two methods are employed in the fabrication of thin magnetic tapes of narrow width for memory applications. During roll-flattening, the material flows laterally without much elongation. The flat-drawing process, on the other hand, results in axial elongation without much change in the lateral direction. Such processing techniques, as preliminary studies have shown,[27] are expected to produce unusual textures and magnetic anisotropies. The results of the experimental studies involving rolling and wire drawing of single crystals to test the theoretical analyses presented here as well as the results of flattening polycrystalline wire materials will be presented in a subsequent paper.

ACKNOWLEDGMENTS

The author expresses sincere thanks to A. T. English, W. F. Hosford, Jr., E. A. Nesbitt, and J. H. Wernick for valuable discussions and review of the manuscript.

[24] P. S. Rudman and B. L. Averbach, Acta Met. 4, 382 (1956).
[25] J. B. Cohen and M. B. Bever, Trans. Met. Soc. AIME **218**, 155 (1960).
[26] M. F. Collins, R. V. Jones, and R. D. Lowde, J. Phys. Soc. Japan **17**, Suppl. B-III, 19 (1962).
[27] G. Y. Chin, L. L. Vanskike, and H. L. Andrews, J. Appl. Phys. Suppl. **35**, 867 (1964).

APPENDIX

Relation between Glide-Shear, Slip Density, and Macrostrain

The "slip density" S, as defined in the CSI analysis, is the average or effective number of dislocations passed per atomic (slip) plane. The glide-shear due to slip can thus be expressed as $\gamma=Sb/d$, where b is the strength of the Burger's vector and d the slip plane spacing. For $\{111\}\ \langle 110\rangle$ slip in face-centered cubic materials, $b=a/\sqrt{2}$ and $d=a/\sqrt{3}$ (a=lattice constant). Hence

$$\gamma=S(\tfrac{3}{2})^{\frac{1}{2}}. \tag{A1}$$

Now the glide shear is related to the macroscopic strain tensor components by the equations[13]

$$\begin{aligned}
\epsilon_{xx}&=\gamma n_x d_x,\\
\epsilon_{yy}&=\gamma n_y d_y,\\
\epsilon_{zz}&=\gamma n_z d_z,\\
\epsilon_{yz}&=(\gamma/2)(n_y d_z+n_z d_y),\\
\epsilon_{zx}&=(\gamma/2)(n_z d_x+n_x d_z),\\
\epsilon_{xy}&=(\gamma/2)(n_x d_y+n_y d_x),
\end{aligned} \tag{A2}$$

where n_x, n_y, n_z are components along the cubic coordinates of a unit vector normal to the slip plane and d_x, d_y, d_z are the components of a unit vector along the slip direction. As an example, take slip on the (111) $[0\bar{1}1]$ system [No. (1) in Table I], $n_x=n_y=n_z=1/\sqrt{3}$, $d_x=0$, $d_y=-1/\sqrt{2}$, $d_z=1/\sqrt{2}$. From Eqs. (A2), we get

$$\begin{aligned}
\epsilon_{xx}&=0,\\
\epsilon_{yy}&=-(\gamma/\sqrt{6}),\\
\epsilon_{zz}&=\gamma/\sqrt{6},\\
\epsilon_{yz}&=0,\\
\epsilon_{zx}&=(\gamma/2)\cdot(1/\sqrt{6}),\\
\epsilon_{xy}&=-(\gamma/2)(1/\sqrt{6}).
\end{aligned} \tag{A3}$$

Finally, by converting γ to S via Eq. (A1),

$$\begin{aligned}
\epsilon_{xx}&=0,\\
\epsilon_{yy}&=-(S_1/2),\\
\epsilon_{zz}&=(S_1/2),\\
\epsilon_{yz}&=0,\\
\epsilon_{zx}&=S_1/4,\\
\epsilon_{xy}&=-(S_1/4),
\end{aligned} \tag{A4}$$

which are the values entered in Table I.